IAI Journals.ASM.org

Brucella canis Is an Intracellular Pathogen That Induces a Lower Proinflammatory Response than Smooth Zoonotic Counterparts

Carlos Chacón-Díaz,[a] Pamela Altamirano-Silva,[a] Gabriela González-Espinoza,[a] María-Concepción Medina,[b] Alejandro Alfaro-Alarcón,[c] Laura Bouza-Mora,[d] César Jiménez-Rojas,[b] Melissa Wong,[a] Elías Barquero-Calvo,[a,b] Norman Rojas,[a] Caterina Guzmán-Verri,[a,b] Edgardo Moreno,[b,e] Esteban Chaves-Olarte[a,b]

Centro de Investigación en Enfermedades Tropicales, Facultad de Microbiología, Universidad de Costa Rica, San José, Costa Rica[a]; Programa de Investigación en Enfermedades Tropicales, Escuela de Medicina Veterinaria, Universidad Nacional, Heredia, Costa Rica[b]; Departamento de Patología, Escuela de Medicina Veterinaria, Universidad Nacional, Heredia, Costa Rica[c]; Laboratorio de Análisis Clínicos, Escuela de Medicina Veterinaria, Universidad Nacional, Heredia, Costa Rica[d]; Instituto Clodomiro Picado, Facultad de Microbiología, Universidad de Costa Rica, San José, Costa Rica[e]

Canine brucellosis caused by *Brucella canis* is a disease of dogs and a zoonotic risk. *B. canis* harbors most of the virulence determinants defined for the genus, but its pathogenic strategy remains unclear since it has not been demonstrated that this natural rough bacterium is an intracellular pathogen. Studies of *B. canis* outbreaks in kennel facilities indicated that infected dogs displaying clinical signs did not present hematological alterations. A virulent *B. canis* strain isolated from those outbreaks readily replicated in different organs of mice for a protracted period. However, the levels of tumor necrosis factor alpha, interleukin-6 (IL-6), and IL-12 in serum were close to background levels. Furthermore, *B. canis* induced lower levels of gamma interferon, less inflammation of the spleen, and a reduced number of granulomas in the liver in mice than did *B. abortus*. When the interaction of *B. canis* with cells was studied *ex vivo*, two patterns were observed, a predominant scattered cell-associated pattern of nonviable bacteria and an infrequent intracellular replicative pattern of viable bacteria in a perinuclear location. The second pattern, responsible for the increase in intracellular multiplication, was dependent on the type IV secretion system VirB and was seen only if the inoculum used for cell infections was in early exponential phase. Intracellular replicative *B. canis* followed an intracellular trafficking route undistinguishable from that of *B. abortus*. Although *B. canis* induces a lower proinflammatory response and has a stealthier replication cycle, it still displays the pathogenic properties of the genus and the ability to persist in infected organs based on the ability to multiply intracellularly.

Brucellosis is a disease of animals and humans caused by members of the genus *Brucella*. Zoonotic species such as *Brucella melitensis*, *Brucella abortus*, and *Brucella suis* are facultative extracellular-intracellular stealthy pathogens that are able to overcome innate immunity at early times of infection (1–3) and at specific stages of adaptive immunity (4, 5). In addition to influencing the immune response, these *Brucella* species are able to circumvent the killing action of professional and nonprofessional phagocytes, transit within phagocytic vacuoles, and replicate extensively within the endoplasmic reticulum of cells (6). These properties allow the bacterium to spread throughout the reticuloendothelial system and promote chronic infection (3).

There are other *Brucella* species that are also relevant pathogens; however, their infective strategies remain unclear and are not in tune with the solid results accepted for the previously mentioned zoonotic brucellae. Among these are *Brucella canis*, the etiological agent of brucellosis in dogs and a zoonotic pathogen (7). This pathogen induces a subclinical infection that may remain undiagnosed for protracted periods (8–10). *B. canis* invades the conjunctiva or the oronasal system or penetrates through the venereal route. Then it is distributed to different organs of the reticuloendothelial system (11). The main clinical consequence of canine brucellosis is abortion in females and epididymitis and prostatitis in male dogs (12, 13). In stud males and bitches, the disease also causes sterility, a factor that causes significant economic losses in commercial kennels. *B. canis* is transmitted through contaminated aborted fetuses, milk, urine, vaginal secretions, and semen.

B. canis is highly specific to dogs and has not been observed in other animals. Nevertheless, the bacterium has the ability to infect humans. Because of the low number of reported human cases, it has been proposed that the bacteria are less infective for humans than are the classical species *B. melitensis*, *B. abortus*, and *B. suis* (3). However, this may be a misconception. In the last decade, there has been a rise in the detection of human infections due to *B. canis* (8, 9). This is due to awareness of the disease in areas where it is endemic and improved diagnoses, as well as increased prevalence of the bacterium in kennel facilities and roaming dogs (10, 14, 15). Therefore, it may be that *B. canis* displays an infectivity similar to that of the other zoonotic brucellae but has the potential to produce no symptoms for prolonged periods (16, 17) by using a stealth strategy.

Histological examination of a dog's infected placenta has sug-

Received 11 August 2015 **Returned for modification** 2 September 2015
Accepted 29 September 2015

Accepted manuscript posted online 5 October 2015

Citation Chacón-Díaz C, Altamirano-Silva P, González-Espinoza G, Medina M-C, Alfaro-Alarcón A, Bouza-Mora L, Jiménez-Rojas C, Wong M, Barquero-Calvo E, Rojas N, Guzmán-Verri C, Moreno E, Chaves-Olarte E. 2015. *Brucella canis* is an intracellular pathogen that induces a lower proinflammatory response than smooth zoonotic counterparts. Infect Immun 83:4861–4870. doi:10.1128/IAI.00995-15.

Editor: C. R. Roy

Address correspondence to Edgardo Moreno, emoreno@racsa.co.cr, or Esteban Chaves-Olarte, esteban.chaves@ucr.ac.cr.

gested that *B. canis* replicates intracellularly (18). In addition, large numbers of *B. canis* bacteria attach to the cell surface; however, studies of cells have failed to demonstrate unambiguously that this bacterium actually replicates intracellularly (19–25). This is significant, since *B. canis* harbors most of the virulence determinants defined for the genus, and the genome of this bacterium is 98 to 99% identical to the genomes of other virulent *Brucella* species. Noticeable differences in relation to other zoonotic *Brucella* species are the structure and biological characteristics of the *B. canis* cell envelope (21–29), features that may influence its virulent behavior.

On the basis of clinical features of natural canine infections, as well as murine experimental brucellosis and *ex vivo* culture models, we propose that *B. canis* uses a stealthier infective strategy than other virulent brucellae. This investigation contributes to the dissection of the pathogenic strategies used by the species of the genus *Brucella* and the understanding of their relative virulence and host specificity.

MATERIALS AND METHODS

Ethics statement. Dogs were voluntary taken by their owners to the Veterinary Hospital of the Veterinary School of the National University of Costa Rica for diagnosis. The owners of the dogs signed a written consent form and were carefully informed regarding all of the medical and diagnostic procedures and informed of the results. Protocols for the use of samples were revised and approved by the Comité Institucional para el Cuido y Uso de los Animales of the Universidad Nacional de Costa Rica (approval SIA 0434-14) and were in agreement with the corresponding law, Ley de Bienestar de los Animales, of Costa Rica (law 7451 on animal welfare).

Protocols for experimentation with mice were revised and approved by the Comité Institucional para el Cuido y Uso de los Animales of the Universidad de Costa Rica (CICUA-47-12) and were in agreement with the corresponding law, Ley de Bienestar de los Animales, of Costa Rica (law 7451 on animal welfare). Mice were housed in the animal building of the Veterinary School, Universidad Nacional, Costa Rica. All of the animals were kept in cages with water and food *ad libitum* under biosafety containment conditions previous to and during the experiment.

Hematological, serological, and clinical chemistry analyses of blood samples. Several cases of epididymitis and abortions were detected in a small number of commercial kennels of golden/Labrador retriever and Pomeranian dogs in Heredia, Costa Rica, between October 2009 and February 2013. Blood and serum samples were recovered from the affected dogs. Hematological, serological, and clinical chemistry tests were performed as described elsewhere (30).

Bacterial strains and constructs. Seventeen isolates of Gram-negative bacteria compatible with *B. canis* were isolated from seminal fluid of stud males, from vaginal swabs of bitches, or from aborted fetuses between 2009 and 2013. The bacterial strains were characterized as *B. canis* by bacteriological analysis (3), molecular Bruce-ladder multiplex PCR assay, and multiplex single nucleotide polymorphism (SNP) detection as reported previously (31, 32). One representative *B. canis* strain named bcanCR12 (here *B. canis*) isolated from a vaginal swab of a Pomeranian bitch after abortion was chosen for biological studies. The results of bacteriological analysis (33), Bruce-ladder multiplex PCR assay (31), multiplex SNP detection (32), and multilocus variable-number tandem-repeat analysis based on 16 loci (MLVA16) (34) were consistent with the *B. canis* genotype.

Brucella strains were grown and maintained as described previously (1). Strains were stored at −80°C in 20% glycerol brain heart infusion. Bacteria were routinely grown in standard tryptic soy broth (TSB) either plain or supplemented with 100 μg/ml ampicillin or 50 μg/ml kanamycin (Km).

Plasmid and chromosomal DNA samples were extracted with the QIAprep spin Miniprep and DNeasy blood and tissue kit (Qiagen GmbH, Hilden, Germany). DNA was purified from agarose gels with the QIAquick gel extraction kit (Qiagen GmbH, Hilden, Germany). Primers were synthetized by Life Technologies Inc. DNA sequencing of fragments was done by Macrogen Inc. (Seoul, Republic of Korea).

A *B. canis virB10* mutant (Δ*virB10*) was constructed as reported elsewhere (35). Briefly, an in-frame deletion was generated by PCR overlap with genomic DNA of *B. canis* as the template. Primers were designed by using the available sequence corresponding to reference strain *B. canis* ATCC 23365. The primers used to generate fragment 1 were virB10-F1 (5′-GACAAGTCGGAAAGCATCGT-3′) and virB10-R2 (5′-TGAAGCC CACGACAAAGAGAAA-3′). Those used to generate fragment 2 were virB10-F3 (5′-TTTCTCTTTGTCGTGGGCTTCAGCTATGCAACCCA GAAGGTC-3′) and virB10-R4 (5′-CTCGCTCGCAGAACACTTC-3′). Both fragments were ligated by PCR overlap with nucleotides virB10-F1 and virB10-R4. The resulting deletion allele was cloned into plasmid pCR2.1 (Life Technologies) and subcloned into the BamHI-XbaI site of suicide plasmid pJQKm. Plasmid pJQKm, containing the deletion allele, was introduced into *B. canis* by conjugation. Colonies corresponding to the integration of the suicide vector into the chromosome were selected with polymyxin B (PxB) and Km resistance; excision of the suicide plasmid led to the construction of the mutant by allelic exchange, and bacteria were selected by PxB and sucrose resistance and Km sensitivity. The resulting colonies were screened with primers virB10-F1 and virB10-R4. Mutant colonies generated a 694-bp fragment, and the parental strain generated a 1,522-bp fragment. The mutation generated resulted in the loss of 71% of the *virB10* open reading frame.

B. canis harboring plasmid pBBR-2-GFP with resistance to Kan and constitutively expressing green fluorescent protein (GFP) (*B. canis*-GFP) was constructed and selected as reported before (36). The expression of GFP was evaluated in bacterial cultures under UV illumination and by fluorescence microscopy as described previously (36). *B. canis* containing a plasmid coding for GFP under the control of the tetracycline-inducible *tetA* promoter (*B. canis*-iGFP) was constructed through conjugation of plasmid pJC45 as described elsewhere (37). With the exception of green fluorescence, the *B. canis*-GFP and *B. canis*-iGFP strains kept the same *in vitro* and *ex vivo* growth and bacteriological characteristics as the parental strain (data not shown).

Virulence assays with mice. Female BALB/c mice (18 to 24 g) were intraperitoneally (i.p.) inoculated with the indicated inoculum of either *B. canis* bcanCR12 or the *B. canis* bcanCR12 Δ*virB10* mutant, and bacterial counts in the spleen, inguinal lymph nodes, liver, and bone marrow were determined at various times as described elsewhere (38, 39). In some experiments, mice were i.p. infected with the indicated inoculum of *B. abortus* 2308. Levels of infection were expressed as mean values and standard deviations SDs ($n = 5$) of the log number of CFU per organ at each time point selected. For histopathological studies, organs from *Brucella*-infected mice were fixed in 10% neutral buffered formalin, processed, and stained with hematoxylin and eosin as described elsewhere (40).

Gentamicin protection assay. Cell infections for estimation of bacterial invasion and replication were performed as described previously (41). Briefly, HeLa cells or Raw 264.7 macrophages were grown to subconfluence in 24-well tissue culture plates. The *B. canis* strains used for cell infections were grown in 20 ml of TSB in glass flasks at 200 rpm as described elsewhere. Flasks were inoculated with 5×10^9 bacteria (42). At different time points on the growth curve, aliquots were used for cell infection. Bacterial inocula taken out at 5, 8, and 12 h correspond to exponential-phase conditions (a, b, and c, respectively), while inocula taken out at 24 and 30 h correspond to stationary-phase conditions (d and e, respectively) (see Fig. 5A). Alternatively, to induce low-aeration conditions, *B. canis* strains were grown in 10 ml of TSB in 50-ml conical plastic tubes at 120 rpm. The multiplicity of infection (MOI) used was adjusted by diluting the bacteria in Eagle's minimal essential medium. Cells were infected with an MOI of either 100 CFU/Raw 264.7 macrophage or 500 CFU/HeLa cell. All of the inocula used to infect cells were serially diluted

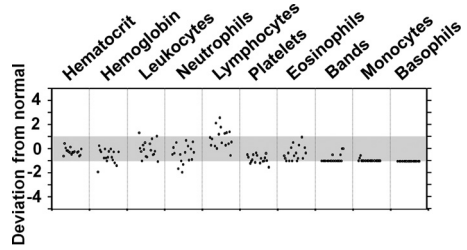

FIG 1 Hematological profiles of infected dogs. The blood cell counts of 17 *B. canis*-infected dogs in a canine brucellosis outbreak in Costa Rica are shown. The gray area demarcates the normal value range of each cell type. The dogs are represented by circles numbered 1 to 17, with number 1 being the farthest to the left in each panel.

and plated in parallel in tryptic soy agar (TSA) to confirm that they contained the same amount of viable bacteria. Plates containing the infected cells were centrifuged at 1,600 rpm at 4°C, incubated for 45 min at 37°C under 5% CO_2, and washed with phosphate-buffered saline. Extracellular bacteria were eliminated by treatment with gentamicin at 100 μg/ml for 1 h, and cells were incubated for the times indicated in the presence of gentamicin at 5 μg/ml. After incubation, cells were lysed by treatment with 0.1% Triton X-100 for 10 min. Aliquots were serially diluted and plated in TSA (Oxoid) and incubated at 37°C for 3 days for determination of CFU counts.

Immunological assays. Cytokine quantitation in the plasma of *Brucella*-infected mice was performed by enzyme-linked immunosorbent assay (eBioscience) according to the manufacturer's instructions. For epifluorescence and confocal microscopy, cells (5×10^5) were grown on 12-mm glass slides and inoculated with *B. canis* strains as described above. GFP expression in *B. canis* iGFP was induced by the addition of 200 nM anhydrotetracycline (ATc; Sigma-Aldrich) prior to immunofluorescence staining as previously described (37). The antibodies used to localize different intracellular compartments were LAMP1 mouse monoclonal antibody H4A3 (Abcam) and rabbit anti-calnexin polyclonal antibody ab75801 (Abcam). Mouse polyclonal antibodies to *B. canis* were used to detect extracellular *Brucella* as reported elsewhere (43). An Alexa Fluor 488-conjugated goat anti-mouse antibody and an Alexa Fluor 594-conjugated anti-mouse antibody (Life Technologies) were used as developing antibodies. Confocal analysis was performed with an Olympus U-TB190 (100×) under oil immersion. Confocal images of 1,024 by 1,024 pixels were acquired with the FV10-AV ver.03.01 software (Olympus) and assembled with Adobe Photoshop CS3 (Adobe Systems, San Jose, CA).

RESULTS

***B. canis*-infected dogs fail to show signs of sepsis or clinical or hematological alterations.** In the course of our clinical studies of infected dogs from which *B. canis* was isolated, we did not detect proinflammatory signs that are characteristic of other bacterial sepsis. Although significant quantities of antibodies against *Brucella* proteins were detected in the sera of 17 infected dogs, the biochemical parameters, including protein concentration, coagulation time, C-reactive protein, and liver and renal functions were within the normal ranges in all of the dogs. Likewise, the blood profiles of the 17 dogs from which *B. canis* strains were isolated were mostly normal, with a few exceptions (Fig. 1). One dog showed mild leukocytosis, while three dogs demonstrated mild neutropenia, probably as a result of lymphocytosis (dogs 7, 11, and 12); 8 of the 17 dogs showed mild lymphocytosis. At the time of sampling, none of the animals had signs of fatigue, displayed an abnormal temperature, or lost weight. These results are consistent with the stealth strategy used by *Brucella* organisms to evade the innate immune response and in agreement with the absence of endotoxemia symptoms in *Brucella* infections (1). Following this, we decided to explore the outcome of *B. canis* infection in the mouse model and in cells.

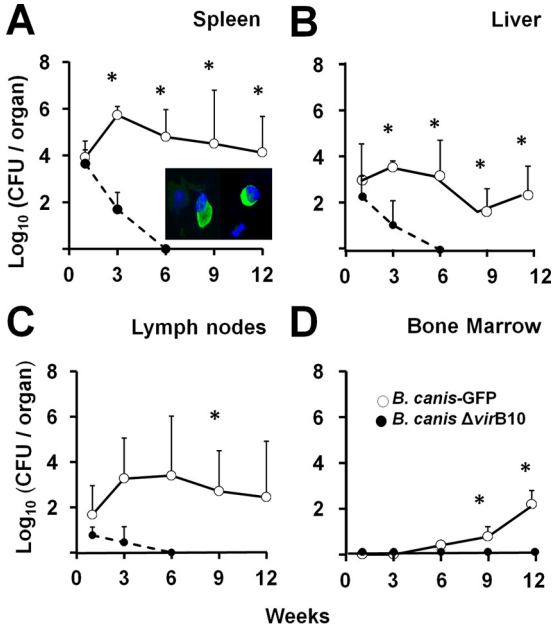

FIG 2 *B. canis* persists and replicates within cells of the reticuloendothelial system. Groups of 30 mice were inoculated i.p. with 10^7 CFU of *B. canis*-GFP or *B. canis* Δ*virB10*-GFP. Groups of five mice were killed at the times indicated to determine the CFU counts in the spleen (A), liver (B), lymph nodes (C), and bone marrow (D). Cells from a spleen infected with *B. canis*-GFP for 21 days were visualized by epifluorescence (inset in panel A). Note the large amounts of *B. canis*-GFP within phagocytic cells. Δ*virB10*-GFP was not observed within resident cells of the spleen. Error bars represent SDs. Data are representative of at least three independent experiments. Statistical significance was calculated by Student *t* test. *, $P < 0.01$.

***B. canis* persists and replicates in the reticuloendothelial system of mice, inducing low proinflammatory responses.** First, we determined the virulence of the *B. canis* strain in groups of five mice inoculated i.p. with 10^7 CFU of *B. canis*-GFP. As expected, the spleen replication curve profile achieved by *B. canis*-GFP was consistent with previous reports (44) (Fig. 2A). Since very little is known regarding organ colonization by *B. canis*, we decided to study the presence of this bacterium in the liver, lymph nodes, and bone marrow (Fig. 2B to D). The replication of *B. canis* in the target organs was somewhat lower than that attained by smooth brucellae and followed a different time course, with a maximal load reached at 3 weeks instead of 1 week (45). However, bacterial loads were maintained and persisted for a protracted period of time in all of the organs tested (Fig. 2). Moreover, the *B. canis* CFU counts in bone marrow increased steadily, coinciding with the persistence and chronicity of the infection (Fig. 2D). Examination of spleen cells from infected mice by immunofluorescence revealed the presence of *B. canis* inside phagocytes, demonstrating the intracellular replication of this bacterium *in vivo* (Fig. 2A, inset). In agreement with a previous report (44), the *B. canis virB10* mutant was already rapidly eliminated from all organs at 6 weeks postinfection (p.i.) and was not recovered from bone marrow or observed inside phagocytic cells (Fig. 2).

Although *B. canis* readily replicates inside phagocytic cells of

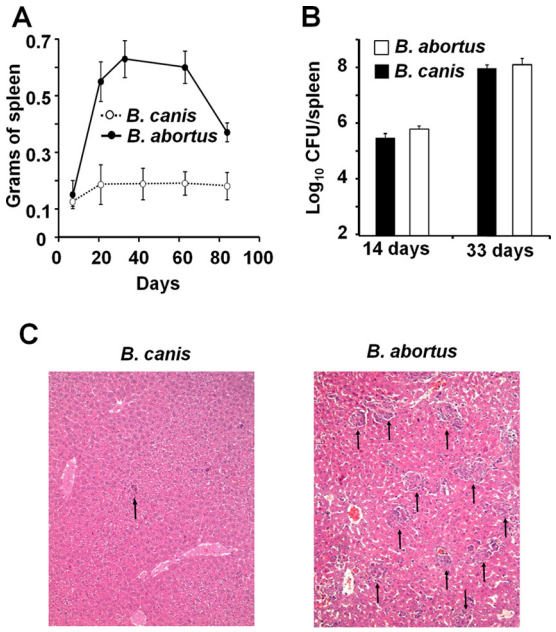

FIG 3 *B. canis* induces a lower proinflammatory response than *B. abortus*. Groups of 30 mice were inoculated i.p. with 10^7 CFU of *B. canis*-GFP or 10^6 CFU of *B. abortus* 2308. Groups of five mice were killed at various times to determine the spleen weight during 12 weeks of infection (A) and bacterial loads at 14 and 33 days p.i. (B). (C) Histological examination of the liver at 2 weeks p.i. with *B. canis* or *B. abortus*. Note that although the *B. canis* and *B. abortus* loads are similar (not statistically significantly different) at 2 weeks p.i., the granulomas (indicated by arrows) are more prominent in the *B. abortus*-infected liver than in the *B. canis*-infected liver. Error bars represent SDs. Data are representative of at least three independent experiments. In panel A, all of the values after 20 days are statistically significantly different ($P < 0.001$).

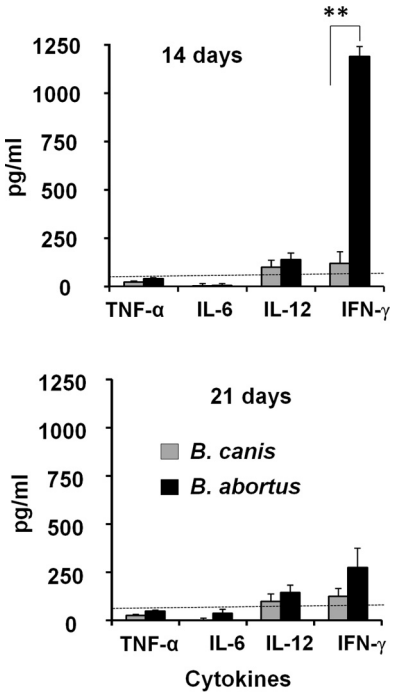

FIG 4 *B. canis* induces a lower cytokine response than *B. abortus*. Groups of 10 mice were inoculated i.p. with 10^7 CFU of *B. canis*-GFP or 10^6 CFU of *B. abortus* 2308. Groups of five mice were killed and bled after 2 and 3 weeks, respectively, to determine serum cytokine levels. Note the small amount of IFN-γ induced after 2 weeks by *B. canis* infection in comparison to that induced by *B. abortus* infection. The dashed lines represent the average background value (SD, <10%). Error bars represent SDs. Data are representative of at least three independent experiments. Statistical significance was calculated by Student *t* test. **, $P < 0.001$.

the spleen, the bacterium barely induced swelling of this organ (Fig. 3A), in contrast to the splenomegaly induced by the same bacterial load of *B. abortus* (Fig. 3B). Histological examination of the liver demonstrated that the number of granulomas induced by *B. canis* infection was considerably lower than that observed in mice infected with *B. abortus* (Fig. 3C). Likewise, histological examination of the spleens of *B. canis*-infected mice also revealed a general milder cellular inflammation than that induced by virulent *B. abortus* (data not shown). In general, the tumor necrosis factor alpha (TNF-α), interleukin-6 (IL-6), and IL-12 cytokine levels of mice infected with *B. canis* after 2 and 3 weeks were low and resembled those induced by *B. abortus* (Fig. 4). An important difference was the level of gamma interferon (IFN-γ), which was rather low in *B. canis* infections, mainly at 2 weeks p.i. (Fig. 4). This is relevant since IFN-γ has been described as the central cytokine during establishment of the adaptive immune response in brucellosis (46). These results demonstrate that *B. canis* induces a lower proinflammatory response in mice than other zoonotic brucellae do (45).

Growth phase state determines the ability of *B. canis* to achieve intracellular replication. Previous works have failed to demonstrate *B. canis* replication *ex vivo* in a variety of cell lines (19–25). We hypothesized that the physiological state of the inoculum would have an impact on the ability of *B. canis* to achieve intracellular replication. To test this hypothesis, we grew the bacteria for 22 h under two different conditions, (i) in 125-ml Erlenmeyer flasks containing 20 ml of TSB at 200 rpm (high aeration) and (ii) in 50-ml conical tubes containing 10 ml of TSB at 120 rpm (low aeration). The inoculum grown under the high-aeration conditions achieved a high bacterial density and was in late exponential phase at the time of cell infection, whereas the inoculum grown under low-aeration conditions achieved a low bacterial density and was in early exponential phase (Fig. 5A). Both inocula were used at the same MOI to infect cells, and their ability to multiply intracellularly was monitored by a gentamicin protection assay. The inoculum prepared under high-aeration conditions was rapidly cleared from cells, with no CFU being recoverable at 48 h (Fig. 5B). On the contrary, the inoculum prepared under low-aeration conditions displayed a curve compatible with intracellular multiplication, with a 10-fold increase from 24 to 48 h (Fig. 5B). These results indicate that the bacterial state on the growth curve influences the ability of *B. canis* to achieve intracellular replication.

To further investigate the permissive replicating conditions of the bacteria, we prepared cell infection inocula taken at different points on the growth curve (Fig. 6A) and then evaluated their intracellular replication competence. In Raw 264.7 macrophages, unambiguous intracellular replication was achieved when the *B. canis* inoculum was at some point of the exponential phase (a, b, c), whereas rapid intracellular clearance was detected when the inoculum was in the stationary phase (Fig. 6B). In epithelial HeLa cells, intracellular replication was achieved only when early-exponential-phase inocula (a, b) were used. Bacteria in the mid-expo-

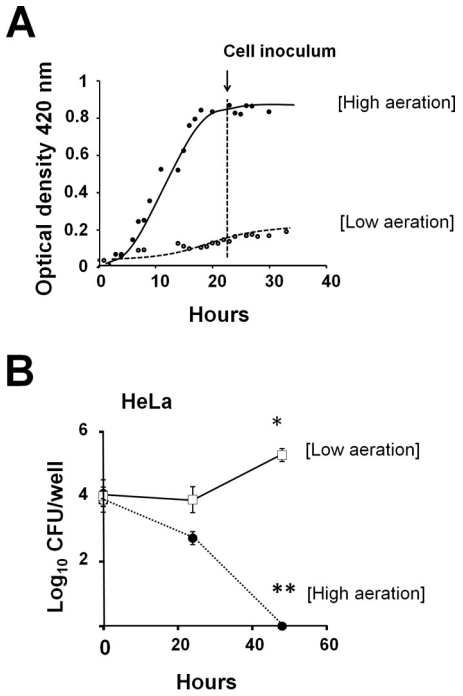

FIG 5 Modulation of the aeration conditions in the bacterial inoculum allows intracellular replication of *B. canis*. (A) *B. canis* cells (5×10^9 CFU) were inoculated and grown for 30 h under high-aeration conditions (20 ml of TSB in 125-ml glass Erlenmeyer flasks, 37°C, 200 rpm) and low-aeration conditions (10 ml of TSB in 50-ml plastic tubes, 37°C, 120 rpm). Aliquots were taken at different times, and the optical densities at 420 nm were measured to determine the growth curves. (B) *B. canis* grown under the conditions indicated in panel A (dashed line) for 22 h was used to prepare the bacterial inoculum. HeLa cells were infected at an MOI of 500 in a gentamicin protection assay. After the incubation times indicated, CFU counts were determined. Error bars represent SDs. Data are representative of at least three independent experiments. Statistical significance was calculated by one-way analysis of variance. *P* values of <0.05 (*) and <0.01 (**) in relation to the corresponding T_0 value of each bacterial condition are indicated.

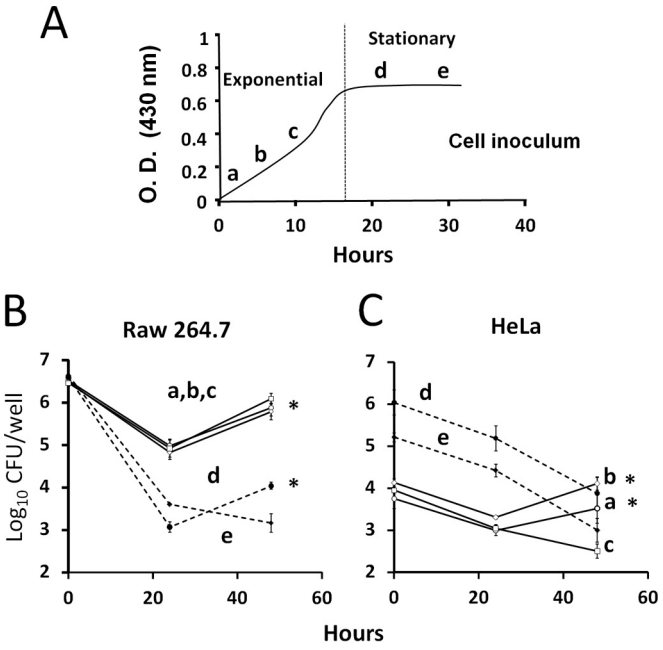

FIG 6 The growth phase of the bacterial inoculum determines the ability of *B. canis* to replicate intracellularly. (A) *B. canis* cells (5×10^9 CFU) were inoculated into 20 ml of TSB in a 125-ml Erlenmeyer flask and incubated at 37°C and 200 rpm for 30 h. Aliquots were taken at 5, 8, and 12 h (a, b, c), representing exponential-phase conditions, and at 24 and 30 h (d and e), representing stationary-phase conditions. O. D., optical density. Bacteria collected under each condition (a to e) were used to inoculate Raw 264.7 macrophages (MOI, 100 CFU) (B) and HeLa cells (MOI, 500 CFU) (C) in a gentamicin protection assay. At the times indicated, the number of CFU per well was determined. Error bars represent SDs. Data are representative of at least three independent experiments. In panels B and C, statistically significant differences between the 24- and 48-h points for each condition were calculated by Student *t* test. *, $P < 0.01$.

nential and stationary phases did not multiply intracellularly (Fig. 6C). The *B. canis virB10* mutant was unable to achieve intracellular multiplication in either cell line under conditions that generate competent replicating *B. canis* (Fig. 7), strengthening the conclusion that we were indeed monitoring intracellular replication.

***B. canis* displays two different cell-associated bacterial patterns.** Once the culture conditions for generating infective *B. canis* were established, we explored the interaction of *B. canis*-GFP with epithelial cells. Two types of cell-associated patterns were observed; the first one corresponded to scattered cell-associated bacteria (Fig. 8A, a to c). This was the predominant pattern observed in the majority of the infected cells at 24 and 48 h p.i. The second pattern corresponded to a phenotype compatible with intracellular replicative bacteria and was characterized by a massive presence of *B. canis*-GFP at a perinuclear location (Fig. 8A, d to f). This pattern was observed in an extremely small proportion of the cells.

The extracellular or intracellular location of *B. canis*-GFP in each pattern was unambiguously determined by adding an anti-*B. canis* antibody to nonpermeabilized cells (Fig. 8B). As expected, the extracellular location of the first pattern was demonstrated since bacteria were accessible to the antibody. Concomitantly, the second pattern indeed corresponded to intracellular replicating bacteria since they were not accessible to the antibody.

Intracellular *B. canis* bacteria are viable and nontoxic. The viability of the scattered cell-associated and intracellular replicative bacteria was determined in HeLa cells infected with *B. canis* expressing GFP under the control of an ATc-inducible promoter. At 48 h p.i., GFP was induced by the addition of ATc and the samples were examined for fluorescence (Fig. 9A). Scattered cell-associated bacteria did not express GFP upon ATc induction, indicating that they were dead bacteria probably killed by gentamicin. In contrast, intracellular replicative bacteria showed robust expression of GFP after the addition of ATc, demonstrating that they are transcriptionally active and thus were viable organisms. As demonstrated for *B. abortus* (1, 41), intracellular replication of *B. canis* was nontoxic, since mitotic cells with a high number of intracellular *B. canis* bacteria were observed (Fig. 9B). This behavior is in clear opposition to mutant rough brucellae, which are highly toxic to cells (47).

The percentage of cells showing intracellular replicative bacteria at 48 h p.i. was determined in monolayers infected with *B. canis* at different points on the growth curve. This percentage was significantly higher in both cells lines when the inoculum was in early phases of the growth curve than when the inoculum was in the late exponential or stationary phase (Fig. 10), showing a strict correlation with the result obtained with the intracellular growth curves (Fig. 6).

***B. canis* replicates within the endoplasmic reticulum and exits through LAMP1-positive vacuoles.** *B. abortus* replicates inside

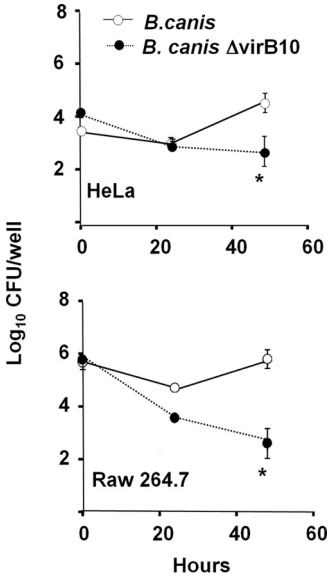

FIG 7 The *B. canis virB10* mutant is unable to replicate in HeLa cells and Raw 264.7 macrophages. Early-exponential-phase (5 h) *B. canis* or *B. canis* Δ*virB10* was used to infect HeLa cells (MOI, 500 CFU) or Raw 264.7 macrophages (MOI, 100 CFU) in a gentamicin protection assay. At the times indicted, the number of CFU per well was determined. Error bars represent SDs. Data are representative of at least three independent experiments. Statistically significant differences between the counts achieved by both strains at 48 h were calculated by Student *t* test. *, $P < 0.01$.

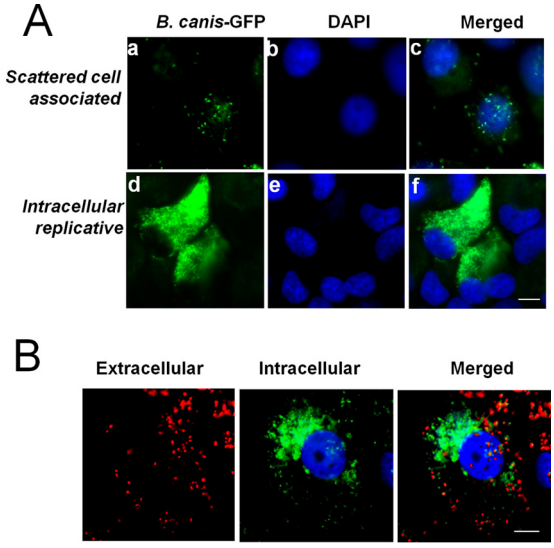

FIG 8 *B. canis* displays two different patterns of interaction with epithelial cells. (A) HeLa cells were infected at an MOI of 500 CFU with an early-exponential-phase inoculum of *B. canis*-GFP grown under low-aeration conditions as indicated in Fig. 5A. After 48 h of incubation, cells were fixed and their nuclei were stained with 4′,6-diamidino-2-phenylindole (DAPI; blue) and visualized by fluorescence microscopy. (A) Two interacting patterns are shown: HeLa cells displaying scattered cell-associated bacteria (a to c) and intracellular replicating bacteria (d and e). (B) At 48 h p.i., living nonpermeabilized HeLa cells were incubated with an antibody to *B. canis* for 30 min at 4°C, followed by an anti-mouse antibody conjugated with Alexa Fluor 594 (Life Technologies). Cells were then fixed, permeabilized, and processed for an immunofluorescence assay. Intracellularly located bacteria are exclusively green (GFP signal), whereas extracellular bacteria are red (anti-*B. canis* signal). Images were contrasted and saturated with the Hue tool to obtain suitable color separation. Scale bars, 5 μm.

the endoplasmic reticulum of its host cell and completes its intracellular cycle by reaching compartments displaying autophagocytic characteristics that allow exodus of the bacterium from the cell (37). We analyzed whether *B. canis* uses the same intracellular pathway. HeLa cells were infected with *B. canis*-GFP grown under conditions that allow intracellular replication. After 48 h of infection, intracellular replicative *B. canis* mostly colocalized with the endoplasmic reticulum marker calnexin, though a small proportion of bacteria was found in LAMP1-positive compartments (Fig. 11A, left side). Despite the low number of cells displaying intracellular replicative bacteria after 72 h of infection, some of them harbored large bacterial clumps inside vacuoles (Fig. 11B) resembling those previously described for *B. abortus* (37). These bacterial clumps were located within large vacuoles devoid of calnexin but surrounded by the LAMP1 marker (Fig. 11A, right side). These LAMP1-positive vacuoles containing bacterial clumps were absent from cells infected with the *B. canis virB10* mutant or *B. canis* bcanCR12 grown under stationary-phase conditions (data not shown).

DISCUSSION

Similar to rough *B. abortus*, *B. melitensis*, and *B. suis* mutants lacking the O-polysaccharide chain of lipopolysaccharide (LPS), *B. canis* displays an exposed oligosaccharide that cross-reacts with core determinants (29). This "rough-like" phenotype also correlates with higher surface hydrophobicity, greater mucousness, and broader adherence to surfaces and cell membranes than those of smooth virulent brucellae (21, 28). Since the rough mutants are attenuated (48), it may be assumed that the slower-replication profile of *B. canis* in the murine model could be due to the absence of the O chain. Nevertheless and *sensu stricto*, *B. canis* is not a rough bacterium and displays significant differences from rough mutants derived from virulent smooth strains. First, it persists in mouse organs, including bone marrow, for a protracted period of time, revealing its ability to maintain a chronic state. Second, *B. canis* is highly infective and virulent for dogs, inducing pathological signs corresponding to brucellosis. Third, *B. canis* is much more resistant than smooth *Brucella* and rough mutants to low pH, complement, hydrogen peroxide, and bactericidal cationic peptides (27), all properties associated with virulence (49, 50). Fourth, *B. canis* induces a lower proinflammatory response than rough *Brucella* mutants in animal models (25), a characteristic linked to its furtive strategy. Fifth, while intracellular *B. canis* is nontoxic to cells, rough *Brucella* mutants induce cell death (47), a trait associated with its intracellular life style. Finally, in contrast to rough mutants but similar to smooth brucellae, *B. canis* penetrates macrophages through lipid rafts (25). Other properties such as iron acquisition and growth metabolic requirements have also been pointed out as relevant differences between *B. canis* and other *Brucella* species (20, 51).

In addition to being highly pathogenic for dogs, *B. canis* is also able to infect humans and eventually cause severe disease (8, 52, 53). Despite this, the bacterium does not induce obvious clinical signs at the onset of infection. The incubation period may last a long time and cause no symptoms before abortion or epididymitis is manifested in dogs. Likewise, experimental infections of monkeys (54) or natural active infections of humans generally last a

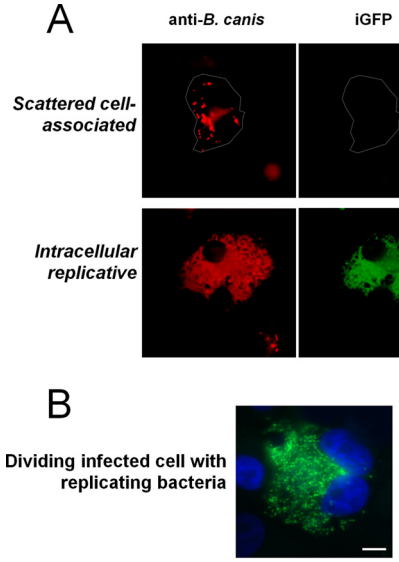

FIG 9 Intracellular *B. canis* bacteria are viable replicating bacteria. (A) HeLa cells were infected at an MOI of 500 with an early-exponential-phase inoculum of *B. canis*-iGFP grown under low-aeration conditions as indicated in Fig. 5A. This strain harbors ATc-inducible GFP. At 48 h p.i., GFP was induced by ATc addition. The cells were then fixed and visualized by fluorescence microscopy. Note that scattered cell-associated bacteria do not display green fluorescence, indicating that they are dead, while the intracellular type of bacterial cells show green fluorescence, indicating active metabolism. (B) Intracellular *B. canis* (green) is shown replicating in dividing cells. Images were contrasted and saturated with the Hue tool to obtain suitable color separation. Scale bars, 10 μm.

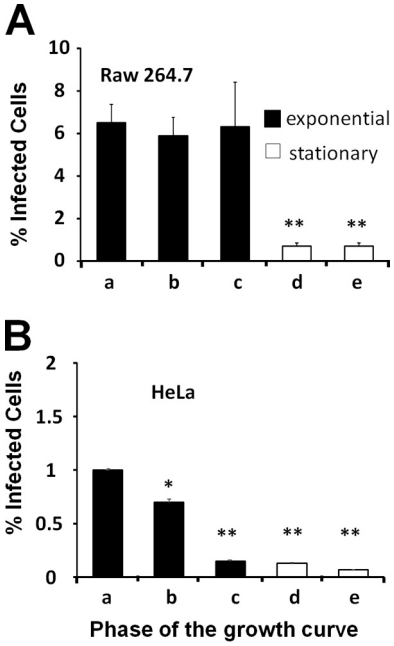

FIG 10 The growth phase of the bacterial inoculum relates to the ability to detect *B. canis* replicating intracellularly. (A) *B. canis* bacterial cells were grown for 30 h in 20 ml of TSB in a glass Erlenmeyer flask at 200 rpm. Aliquots were taken out at 5, 8, and 12 h (a, b, and c, respectively), representing exponential-phase conditions, and at 24 and 30 h (d and e, respectively), representing stationary-phase conditions, as indicated in the legend to Fig. 6A. Bacteria from each condition (a to e) were used to inoculate cells. The proportions of Raw 264.7 macrophages (B) and HeLa epithelial cells (C) displaying intracellular replicative *B. canis* at 48 h p.i. are shown. Error bars represent SDs. Data are representative of at least three independent experiments. The statistical significance of differences was calculated by Student *t* test. *, $P < 0.01$; **, $P < 0.001$ (in relation to inoculum a [early exponential phase]).

long time without any pyogenic signs (16, 17) until the disease is finally manifested. In experimental murine brucellosis, persistence is clearly demonstrated by bone marrow infection at later times, with low cytokine production.

It is therefore evident that *B. canis*, like other virulent brucellae (1, 2), follows a stealth strategy to evade the immune response of its host, mainly during the first stages of infection. However, *B. canis* seems to display even stealthier behavior, since it promotes a lower and slower proinflammatory response than that induced by the classical zoonotic smooth *Brucella* species. Despite inducing significant pathology in dogs, *B. canis* barely promotes altered hematological profiles or signs of endotoxicity. The milder inflammation of the target organs and the smaller amounts of IFN-γ induced during *B. canis* infections of mice are in agreement with this proposal. This claim is also endorsed by works demonstrating rather low cytokine induction, even with heat-killed *B. canis* or *B. canis* Δ*virB* mutant bacteria (44, 55); absence of macrophage activation (25); and the lower reactive oxygen species response in *B. canis*-infected humans than in those infected with smooth *Brucella* species (56–58).

As in other brucellae, the stealth strategy followed by *B. canis* seems to be linked to the absence of recognition of putative pathogen-associated molecular patterns (PAMPs) as a result of significant changes in the cell envelope components that also allow the bacterium to persist for a longer time (21, 25–29). Moreover, a large proportion of the *B. canis* infecting bacteria that remain extracellularly located are killed, exposing putative intracellular PAMPs; still, the cytokine levels remain low. This phenomenon is reminiscent of the absence of cytokine production after the administration of killed *B. abortus* to mice (1).

In addition to the low proinflammatory response behavior of *B. canis*, the extremely low percentage of individual bacterial cells able to achieve productive intracellular replication, even under optimal *in vitro* growth conditions, seems to be a crucial part of the strategy used by *B. canis*. This low rate of intracellular replication, which still takes place in the same compartments described for smooth brucellae, might contribute to the avoidance of strong activation of the immune response and allow *B. canis* to slowly colonize various organs before effective adaptive immunity develops.

The relevance of the *virB* operon for *B. canis* virulence has been demonstrated before in the mouse model (44), but its participation in the intracellular lifestyle of this species has not. As is the case with other *Brucella* species, this system is an essential component of the achievement of successful intracellular replication of *B. canis* within the endoplasmic reticulum of host cells. We demonstrated that in order to achieve intracellular survival competence, the bacterium requires restricted culture conditions and needs to be in early stages of the growth curve. These conditions may allow the regulation of this injection machinery, as well as other systems important for virulence that impact the expression of the *virB* operon, such as the transcriptional regulator VjbR and the two-component system BvrR/BvrS, before cell infection (59, 60). Alternatively, *B. canis* in late stages of the growth curve may secrete metabolites that would inhibit intracellular replication. Even

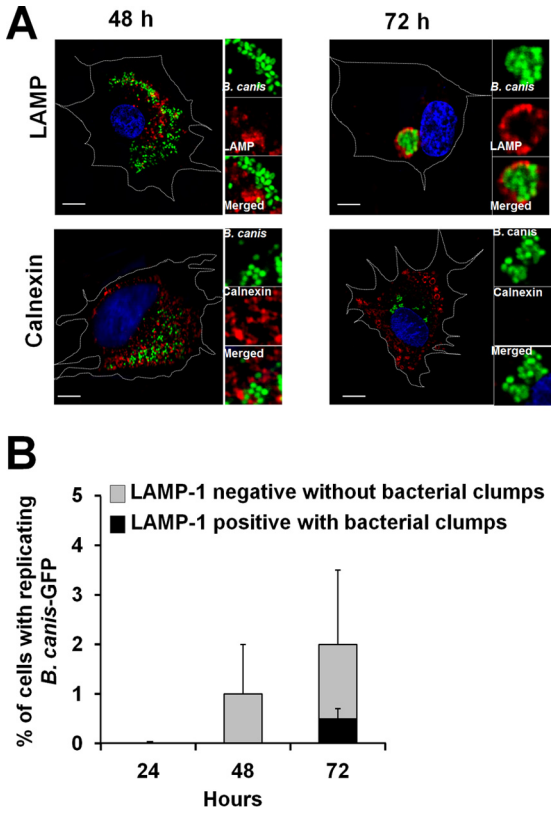

FIG 11 *B. canis* transits through the endoplasmic reticulum and reaches autophagosome-like vacuoles at late times postinfection. (A) HeLa cells were infected at an MOI of 500 with an early-exponential-phase inoculum of *B. canis*-GFP grown under low-aeration conditions as indicated in Fig. 5A. At the times indicated, cells were processed for an immunofluorescence assay with antibodies to LAMP1 (red, top) or calnexin (red, bottom). Cells were visualized by confocal microscopy. Scale bars, 5 μm. (B) Percentages of cells displaying intracellular replicative *B. canis* (gray bars) and clumps of bacteria surrounded by LAMP1 (black bars). Images were contrasted and saturated with the Hue tool to obtain suitable color separation. Error bars represents SDs. Data are representative of at least three independent experiments.

though our purpose was not to dissect in molecular and cellular detail the process by which *B. canis* becomes prone to achieve replication in cultured cells, the protocols designed allow further investigation of this relevant mechanism of control of intracellular replication.

The host constraint and cell envelope properties of *B. canis* are partially shared with *Brucella ovis*, an intracellular pathogenic species restricted to sheep that is also devoid of *N*-formylperosamine polysaccharides (61). However, *B. canis* departs from *B. ovis* in many respects, including the antigenicity of its LPS, its host preference, and its zoonotic potential (3, 29). In addition, genetic analysis has indicated that *B. canis* and *B. ovis* emerged as two independent *Brucella* lineages (62). Indeed, the absence of the O-polysaccharide chain linked to the rough LPS corresponds to convergent evolution rather than a common origin of these two species, since *B. ovis* carries a frameshift in *wbkF* (63) and a GI-2 deletion (64) while *B. canis* conserves GI-2 but carries a deletion overlapping *wbkD* and *wbkF* (63).

There is a long history of the coexistence of dogs and humans (65). Still, the reported number of human cases of *B. canis* brucellosis is low. From a practical perspective, it should be noted that the stealthier strategy and the long incubation period in the absence of obvious clinical signs make it difficult to detect *B. canis* infection. As has been pointed out before, this is aggravated by deficiencies in testing, mainly because of a lack of available diagnostic capabilities that leads to underestimation of the disease (9). As a consequence, a great many infections may go undiagnosed. In addition, the low socioeconomic conditions under which many canine infections have been detected may hamper the diagnosis of the disease, as previously proposed (52).

In conclusion, there are several reports of *Brucella* organisms not replicating intracellularly in *ex vivo* assays (21, 22, 66, 67). In light of the results presented here, the absence of intracellular replication of *Brucella* bacteria in cultured cells should be taken cautiously. There is also an urgent need for the standardization of infection protocols in order to decipher and compare the vast number of published results in brucellosis research.

ACKNOWLEDGMENTS

We thank Daphnne Garita (Universidad Nacional, Heredia, Costa Rica) for her help in the serological diagnosis of *B. canis* infections. We also thank Nazareth Ruiz-Villalobos (Universidad Nacional, Heredia, Costa Rica) for helping in the MLVA16 characterization of the *B. canis* isolates. We also thank Jean Celli (University of Washington) for providing the GFP-inducible plasmid.

This work was funded by Fondos de Recursos del Sistema FEES/CONARE projects 803-B4-654 and 803-B5-653 (www.conare.ac.cr); Red Temática de Brucelosis, Vice-Presidency for Research, University of Costa Rica, project 803-B3-761 (www.vinv.ucr.ac.cr); The National Council of Science and Technology of Costa Rica through FORINVES grant FV-0004-13 (www.conicit.go.cr); and The International Center for Genomic Engineering and Biotechnology, contract CRP/12/007 (www.icgeb.trieste.it). Fellowship support for María Concepción Medina from the Teasdale-Corti Project, Honduras-Canada, and fellowship support for Carlos Chacón Díaz from SEP-CONARE are gratefully acknowledged. The funders had no role in study design, data collection and analysis, the decision to publish, or preparation of the manuscript.

REFERENCES

1. **Barquero-Calvo E, Chaves-Olarte E, Weiss DS, Guzmán-Verri C, Chacón-Díaz C, Rucavado A, Moriyón I, Moreno E.** 2007. *Brucella abortus* uses a stealthy strategy to avoid activation of the innate immune system during the onset of the infection. PLoS One **2:**e631. http://dx.doi.org/10.1371/journal.pone.0000631.
2. **Martirosyan A, Moreno E, Gorvel JP.** 2011. An evolutionary strategy for a stealthy intracellular *Brucella* pathogen. Immunol Rev **240:**211–234. http://dx.doi.org/10.1111/j.1600-065X.2010.00982.x.
3. **Moreno E, Moriyón I.** 2006. The genus *Brucella*, p 315–456. *In* Dworkin M, Falkow S, Rosenberg E, Schleifer K-H, Stackebrant E (ed), The prokaryotes, vol 5. Springer Verlag, New York, NY.
4. **Martirosyan A, Gorvel JP.** 2013. *Brucella* evasion of adaptive immunity. Future Microbiol **8:**147–154. http://dx.doi.org/10.2217/fmb.12.140.
5. **Xavier MN, Winter MG, Spees AM, Nguyen K, Atluri VL, Silva TM, Bäumler AJ, Müller W, Santos RL, Tsolis RM.** 2013. $CD4^+$ T cell-derived IL-10 promotes *Brucella abortus* persistence via modulation of macrophage function. PLoS Pathog **9:**e1003454. http://dx.doi.org/10.1371/journal.ppat.1003454.
6. **von Bargen K, Gorvel JP, Salcedo S.** 2012. Internal affairs: investigating the *Brucella* intracellular lifestyle. FEMS Microbiol Rev **36:**533–562. http://dx.doi.org/10.1111/j.1574-6976.2012.00334.x.
7. **Swenson RM, Carmichael LE, Cundy KR.** 1972. Human infection with *Brucella canis*. Ann Intern Med **76:**435–438. http://dx.doi.org/10.7326/0003-4819-76-3-435.
8. **Lucero NE, Jacob NO, Ayala SM, Escobar GI, Tuccillo P, Jacques I.** 2005. Unusual clinical presentation of brucellosis caused by *Brucella canis*. J Med Microbiol **54:**505–508. http://dx.doi.org/10.1099/jmm.0.45928-0.
9. **Lucero NE, Corazza R, Almuzara MN, Reynes E, Escobar GI, Boeri**

E, Ayala SM. 2010. Human *Brucella canis* outbreak linked to infection in dogs. Epidemiol Infect **138:**280–285. http://dx.doi.org/10.1017/S0950268809990525.
10. **Lucero NE, Escobar GI, Ayala SM, Jacob N.** 2005. Diagnosis of human brucellosis caused by *Brucella canis*. J Med Microbiol **54:**457–461. http://dx.doi.org/10.1099/jmm.0.45927-0.
11. **Carmichael LE, Joubert JC.** 1988. Transmission of *Brucella canis* by contact exposure. Cornell Vet **78:**63–73.
12. **Carmichael LE, Kenney RM.** 1968. Canine abortion caused by *Brucella canis*. J Am Vet Med Assoc **152:**605–616.
13. **Moore JA, Kakuk TJ.** 1969. Male dogs naturally infected with *Brucella canis*. J Am Vet Med Assoc **155:**1352–1358.
14. **Ayala SM, Hasan DB, Celestino CA, Escobar GI, Zhao DM, Lucero NE.** 2014. Validation of a simple universal IELISA for the diagnosis of human brucellosis. Eur J Clin Microbiol Infect Dis **33:**1239–1246. http://dx.doi.org/10.1007/s10096-014-2066-2.
15. **Di D, Cui B, Wang H, Zhao H, Piao D, Tian L, Tian G, Kang J, Mao X, Zhang X, Du P, Zhu L, Zhao Z, Mao L, Yao W, Guan P, Fan W, Jiang H.** 2014. Genetic polymorphism characteristics of *Brucella canis* isolated in China. PLoS One **9:**e84862. http://dx.doi.org/10.1371/journal.pone.0084862.
16. **Olivera M, Di-Lorenzo C.** 2009. Aislamiento de *Brucella canis* en un humano conviviente con caninos infectados. Informe de un caso. Colomb Med **40:**218–220.
17. **Polt SS, Dismukes WE, Flint A, Schaefer J.** 1982. Human brucellosis caused by *Brucella canis*: clinical features and immune response. Ann Intern Med **97:**717–719. http://dx.doi.org/10.7326/0003-4819-97-5-717.
18. **Gyuranecz M, Szeredi L, Rónai Z, Dénes B, Dencso L, Dán Á Pálmai N, Hauser Z, Lami E, Makrai L, Erdélyi K, Jánosi S.** 2011. Detection of *Brucella canis*-induced reproductive diseases in a kennel. J Vet Diagn Invest **23:**143–147. http://dx.doi.org/10.1177/104063871102300127.
19. **Caron E, Liautard JP, Köhler S.** 1994. Differentiated U937 cells exhibit increased bactericidal activity upon LPS activation and discriminate between virulent and avirulent *Listeria* and *Brucella* species. J Leukoc Biol **56:**174–181.
20. **Eskra L, Covert J, Glasner J, Splitter G.** 2012. Differential expression of iron acquisition genes by *Brucella melitensis* and *Brucella canis* during macrophage infection. PLoS One **7:**e31747. http://dx.doi.org/10.1371/journal.pone.0031747.
21. **Detilleux PG, Deyoe BL, Cheville NF.** 1990. Entry and intracellular location of *Brucella* spp. in Vero cells: fluorescence and electron microscopy. Vet Pathol **27:**317–328.
22. **Rittig MJ, Kauffmann A, Robins A, Shaw B, Sprenger H, Gemsa D, Foulongne V, Rouot B, Dornand J.** 2003. Smooth and rough lipopolysaccharide types of *Brucella* induce different intracellular trafficking and cytokine/chemokine release in human monocytes. J Leukoc Biol **74:**1045–1055. http://dx.doi.org/10.1189/jlb.0103015.
23. **Delpino MV, Fossati CA, Baldi PC.** 2009. Proinflammatory response of human osteoblastic cell lines and osteoblast-monocyte interaction upon infection with *Brucella* spp. Infect Immun **77:**984–995. http://dx.doi.org/10.1128/IAI.01259-08.
24. **Ferrero MC, Fossati CA, Baldi PC.** 2009. Smooth *Brucella* strains invade and replicate in human lung epithelial cells without inducing cell death. Microbes Infect **11:**476–483. http://dx.doi.org/10.1016/j.micinf.2009.01.010.
25. **Martín-Martín AI, Vizcaíno N, Fernández-Lago L.** 2010. Cholesterol, ganglioside GM1 and class A scavenger receptor contribute to infection by *Brucella ovis* and *Brucella canis* in murine macrophages. Microbes Infect **12:**246–251. http://dx.doi.org/10.1016/j.micinf.2009.12.008.
26. **Dees SB, Hollis DG, Weaver RE, Moss CW.** 1981. Cellular fatty acids of *Brucella canis* and *Brucella suis*. J Clin Microbiol **14:**111–112.
27. **Martín-Martín Al, Sancho P, Tejedor C, Fernández-Lago L, Vizcaíno N.** 2011. Differences in the outer membrane-related properties of the six classical *Brucella* species. Vet J **189:**103–105. http://dx.doi.org/10.1016/j.tvjl.2010.05.021.
28. **Martínez de Tejada G, Moriyón I.** 1993. The outer membranes of *Brucella* spp. are not barriers to hydrophobic permeants. J Bacteriol **175:**5273–5275.
29. **Moreno E, Jones LM, Berman DT.** 1984. Immunochemical characterization of rough *Brucella* lipopolysaccharides. Infect Immun **43:**779–782.
30. **Lumsden JH, Mullen K, McSherry BJ.** 1979. Canine hematology and biochemistry reference values. Can J Comp Med **43:**125–131.
31. **López-Goñi I, García-Yoldi D, Marín CM, de Miguel MJ, Barquero-Calvo E, Guzmán-Verri Albert D, Garin-Bastuji B.** 2011. New Bruce-ladder multiplex PCR assay for the biovar typing of *Brucella suis* and the discrimination of *Brucella suis* and *Brucella canis*. Vet Microbiol **154:**152–155. http://dx.doi.org/10.1016/j.vetmic.2011.06.035.
32. **Scott J, Koylass MS, Stubberfield MR, Whatmore A.** 2007. Multiplex assay based on single-nucleotide polymorphism for rapid identification of *Brucella* isolates at the species level. Appl Environ Microbiol **73:**7331–7337. http://dx.doi.org/10.1128/AEM.00976-07.
33. **Alton GG, Jones L, Verger A.** 1988. Techniques for the brucellosis laboratory. Institut National de la Recherche Agronomique, Paris, France.
34. **Le Flèche P, Jacques I, Grayon M, Al Dahouk S, Bouchon P, Denoeud F, Nockler K, Neubauer H, Guilloteau L, Vergnaud G.** 2006. Evaluation and selection of tandem repeat loci for a Brucella MLVA typing assay. BMC Microbiol **6:**9. http://dx.doi.org/10.1186/1471-2180-6-9.
35. **Conde-Álvarez R, Grilló MJ, Salcedo de Miguel S, Fugier MJ, Gorvel E, Moriyón JP, Iriarte I, M.** 2006. Synthesis of phosphatidylcholine, a typical eukaryotic phospholipid, is necessary for full virulence of the intracellular bacterial parasite *Brucella abortus*. Cell Microbiol **8:**1322–1335. http://dx.doi.org/10.1111/j.1462-5822.2006.00712.x.
36. **Chacón-Díaz C, Muñoz-Rodríguez M, Barquero-Calvo E, Guzmán-Verri C, Chaves-Olarte E, Grilló MJ, Moreno E.** 2011. The use of green fluorescent protein as a marker for Brucella vaccines. Vaccine **29:**577–582. http://dx.doi.org/10.1016/j.vaccine.2010.09.109.
37. **Starr T, Child R, Wehrly TD, Hansen B, Hwang S, López-Otin C, Virgin HW, Celli J.** 2012. Selective subversion of autophagy complexes facilitates completion of the intracellular cycle. Cell Host Microbe **11:**33–45. http://dx.doi.org/10.1016/j.chom.2011.12.002.
38. **Barquero-Calvo E, Chacón-Díaz C, Chaves-Olarte E, Moreno E.** 2013. Bacterial counts in spleen. Bio Protoc **3:**e954. http://www.bio-protocol.org/e954.
39. **Grilló MJ, Manterola L, de Miguel MJ, Muñoz P, Blasco JM, Moriyón I, López-Goñi.** 2006. Increases of efficacy as vaccine against *Brucella abortus* infection in mice by simultaneous inoculation with avirulent smooth bvrS/bvrR and rough wbkA mutants. Vaccine **24:**2910–2916. http://dx.doi.org/10.1016/j.vaccine.2005.12.038.
40. **Aughey E, Frye FL.** 2001. Comparative veterinary histology: with clinical correlates. Manson Publishing, London, England.
41. **Chaves-Olarte E, Guzmán-Verri C, Méresse S, Desjardins M, Pizarro-Cerdá J, Badilla J, Gorvel JP, Moreno E.** 2002. Activation of Rho and Rab GTPases dissociates *Brucella abortus* internalization from intracellular trafficking. Cell Microbiol **4:**663–676. http://dx.doi.org/10.1046/j.1462-5822.2002.00221.x.
42. **Martínez-Núñez C, Altamirano-Silva P, Alvarado-Guillén F, Moreno E, Guzmán-Verri C, Chaves-Olarte E.** 2010. The two-component system BvrR/BvrS regulates the expression of the type IV secretion system VirB in *Brucella abortus*. J Bacteriol **192:**5603–5608. http://dx.doi.org/10.1128/JB.00567-10.
43. **Pizarro-Cerdá J, Moreno E, Sanguedolce V, Mege JL, Gorvel JP.** 1998. Virulent *Brucella abortus* prevents lysosome fusion and is distributed within autophagosome-like compartments. Infect Immun **66:**2387–2392.
44. **Palomares-Resendiz E, Arellano-Reynoso B, Hernández-Castro R, Tenorio-Gutiérrez V, Salas-Téllez E, Súarez-Güemes F, Díaz-Aparicio E.** 2012. Immunogenic response of *Brucella canis virB10* and *virB*11 mutants in a murine model. Front Cell Infect Microbiol **2:**35. http://dx.doi.org/10.3389/fcimb.2012.00035.
45. **Grilló MJ, Blasco JM, Gorvel JP, Moriyón I, Moreno E.** 2012. What have we learned from brucellosis in the mouse model? Vet Res **43:**29. http://dx.doi.org/10.1186/1297-9716-43-29.
46. **Baldwin CL, Goenka R.** 2006. Host immune responses to the intracellular bacteria *Brucella*: does the bacteria instruct the host to facilitate chronic infection? Crit Rev Immunol **26:**407–442. http://dx.doi.org/10.1615/CritRevImmunol.v26.i5.30.
47. **Pei J, Turse JE, Wu Q, Ficht TA.** 2006. *Brucella abortus* rough mutants induce macrophage oncosis that requires bacterial protein synthesis and direct interaction with the macrophage. Infect Immun **74:**2667–2675. http://dx.doi.org/10.1128/IAI.74.5.2667-2675.2006.
48. **González D, Grilló MJ, de Miguel MJ, Ali T, Arce-Gorvel V, Delrue RM, Conde-Álvarez R, Muñoz P, López-Goñi I, Iriarte M, Marín CM, Weintraub A, Widmalm G, Zygmunt M, Letesson JJ, Gorvel JP, Blasco JM, Moriyón I.** 2008. Brucellosis vaccines: assessment of *Brucella melitensis* lipopolysaccharide rough mutants defective in core and O-polysaccharide synthesis and export. PLoS One **3:**e2760. http://dx.doi.org/10.1371/journal.pone.0002760.

49. **Martínez de Tejada G, Pizarro-Cerdá J, Moreno E, Moriyón I.** 1995. The outer membranes of *Brucella* spp. are resistant to bactericidal cationic peptides. Infect Immun **63:**3054–3061.
50. **Freer E, Moreno E, Moriyón I, Pizarro-Cerdá J, Weintraub A, Gorvel JP.** 1996. *Brucella-Salmonella* lipopolysaccharide chimeras are less permeable to hydrophobic probes and more sensitive to cationic peptides and EDTA than are their native *Brucella* sp. counterparts. J Bacteriol **178:** 5867–5876.
51. **Jenner DC, Dassa E, Whatmore AM, Atkins HS.** 2009. ATP-binding cassette systems of *Brucella*. Comp Funct Genomics **2009:**354649. http://dx.doi.org/10.1155/2009/354649.
52. **Krueger WS, Lucero NE, Brower A, Heil GL, Gray GC.** 2014. Evidence for unapparent *Brucella canis* infections among adults with occupational exposure to dogs. Zoonoses Public Health **61:**509–518. http://dx.doi.org/10.1111/zph.12102.
53. **Marzetti S, Carranza C, Roncallo M, Escobar GI, Lucero NE.** 2013. Recent trends in human *Brucella canis* infection. Comp Immunol Microbiol Infect Dis **36:**55–61. http://dx.doi.org/10.1016/j.cimid.2012.09.002.
54. **Percy D, Egwu HI, Jonas AM.** 1972. Experimental *Brucella canis* infection in the monkey (*Macaca arctoides*). Can J Comp Med **36:**221–225.
55. **Clausse M, Díaz AG, Ghersi G, Zylberman V, Cassataro J, Giambartolomei GH, Goldbaum FA, Estein SM.** 2013. The vaccine candidate BLSOmp31 protects mice against *Brucella canis* infection. Vaccine **31:** 6129–6135. http://dx.doi.org/10.1016/j.vaccine.2013.07.041.
56. **Karsen H, Karahocagil MK, Akdeniz H, Ceylan MR, Binici I, Selek S, Celik H.** 2011. Serum paraoxonase and arylesterase activities and oxidant status in patients with brucellosis. Afr J Microbiol Res **5:**1701–1706. http://dx.doi.org/10.5897/AJMR11.438.
57. **Serefhanoglu K, Taskin A, Turan H, Timurkaynak FE, Arslan H, Erel O.** 2009. Evaluation of oxidative status in patients with brucellosis. Braz J Infect Dis **13:**249–251. http://dx.doi.org/10.1590/S1413-86702009000400001.
58. **Ustaa M, Arasb Z, Tasc A.** 2012. Oxidant and antioxidant parameters in patients with *Brucella canis*. Clin Biochem **45:**366–367. http://dx.doi.org/10.1016/j.clinbiochem.2011.12.028.
59. **Sola-Landa A, Pizarro-Cerdá J, Grilló MJ, Moreno E, Moriyón I, Blasco JM, Gorvel JP, López-Goñi I.** 1998. A two-component regulatory system playing a critical role in plant pathogens and endosymbionts is present in *Brucella abortus* and controls cell invasion and virulence. Mol Microbiol **29:**125–138. http://dx.doi.org/10.1046/j.1365-2958.1998.00913.x.
60. **Uzureau S, Godefroid M, Deschamps C, Lemaire J, De Bolle X, Letesson JJ.** 2007. Mutations of the quorum sensing-dependent regulator VjbR lead to drastic surface modifications in *Brucella melitensis*. J Bacteriol **189:** 6035–6047. http://dx.doi.org/10.1128/JB.00265-07.
61. **Silva TM, Mol JP, Winter MG, Atluri V, Xavier MN, Pires SF, Paixão TA, Andrade HM, Santos RL, Tsolis RM.** 2014. The predicted ABC transporter AbcEDCBA is required for type IV secretion system expression and lysosomal evasion by *Brucella ovis*. PLoS One **9:**e114532. http://dx.doi.org/10.1371/journal.pone.0114532.
62. **Zygmunt MS, Blasco JM, Letesson JJ, Cloeckaert A, Moriyon I.** 2009. DNA polymorphism analysis of *Brucella* lipopolysaccharide genes reveals marked differences in O-polysaccharide biosynthetic genes between smooth and rough *Brucella* species and novel species-specific markers. BMC Microbiol **9:**92. http://dx.doi.org/10.1186/1471-2180-9-92.
63. **Vizcaíno N, Caro-Hernandez P, Cloeckaert A, Fernandez-Lago L.** 2004. DNA polymorphism in the omp25/omp31 family of *Brucella* spp. identification of a 1.7-kb inversion in *Brucella cetaceae* and of a 15.1-kb genomic island, absent from *Brucella ovis*, related to the synthesis of smooth lipopolysaccharide. Microbes Infect **6:**821–824. http://dx.doi.org/10.1016/j.micinf.2004.04.009.
64. **Mancilla M, López-Goñi I, Moriyón I, Zárraga AM.** 2010. Genomic island 2 is an unstable genetic element contributing to *Brucella* lipopolysaccharide spontaneous smooth-to-rough dissociation. J Bacteriol **192:** 6346–6351. http://dx.doi.org/10.1128/JB.00838-10.
65. **Thalmann O, Shapiro B, Cui P, Schuenemann VJ, Sawyer SK, Greenfield DL, Germonpré MB, Sablin MV, López-Giráldez F, Domingo-Roura X, Napierala H, Uerpmann HP, Loponte DM, Acosta AA, Giemsch L, Schmitz RW, Worthington B, Buikstra JE, Druzhkova A, Graphodatsky AS, Ovodov ND, Wahlberg N, Freedman AH, Schweizer RM, Koepfli KP, Leonard JA, Meyer M, Krause J, Pääbo S, Green RE, Wayne RK.** 2013. Complete mitochondrial genomes of ancient canids suggest a European origin of domestic dogs. Science **342:**871–874. http://dx.doi.org/10.1126/science.1243650.
66. **Maquart M, Zygmunt MS, Cloeckaert A.** 2009. Marine mammals *Brucella* isolates with different genomic characteristics display a differential response when infecting human macrophages in culture. Microbes Infect **11:**361–366. http://dx.doi.org/10.1016/j.micinf.2008.12.012.
67. **Larsen AK, Nymo IH, Briquemont B, Sorensen KK, Godfroid J.** 2013. Entrance and survival of *Brucella pinnipedialis* hooded seal strain in human macrophages and epithelial cells. PLoS One **8:**e84861. http://dx.doi.org/10.1371/journal.pone.0084861.